CrystEngComm

Repurposing of the anti-HIV drug Emtricitabine as a hydrogen-bonded cleft for bipyridines via cocrystallization

Journal:	*CrystEngComm*
Manuscript ID	CE-COM-03-2020-000474.R1
Article Type:	Communication
Date Submitted by the Author:	20-Feb-2020
Complete List of Authors:	Campillo-Alvarado, Gonzalo; University of Iowa, Department of Chemistry Keene, Elizabeth; University of Iowa, Department of Chemistry Swenson, Dale; University of Iowa, Chemistry MacGillivray, Len; University of Iowa, Department of Chemistry

COMMUNICATION

Repurposing of the anti-HIV drug Emtricitabine as a hydrogen-bonded cleft for bipyridines *via* cocrystallization

Received 00th January 20xx,
Accepted 00th January 20xx

DOI: 10.1039/x0xx00000x

Gonzalo Campillo-Alvarado, Elizabeth A. Keene, Dale C. Swenson and Leonard R. MacGillivray*

We report supramolecular repurposing of Emtricitabine (FTC, trade name: Emtriva®), a blockbuster FDA-approved anti-HIV agent. FTC is revealed to act as a hydrogen-bonded cleft for bipyridine recognition. The supramolecular repurposing is realized by the generation of four cocrystals through liquid-assisted grinding. The clefts comprise discrete three-component assemblies sustained by a combination of hydrogen bonds and π···π interactions.

While the repurposing of pharmaceutical ingredients (APIs) is an important business model in drug development, the act of repurposing molecules for other applications (e.g. materials science) remains largely unexplored.[1] Generally, the tactic consists in finding new uses of existing molecules applied to molecular and/or supramolecular chemistry. Applications in the supramolecular domain are extremely rare and constitute sustainable research with promising applications. Diao, for example, has just applied supramolecular repurposing of DNA-binding agents to develop hydrogen-bonded organic semiconductors.[2]

Here, we describe supramolecular repurposing of the FDA-approved anti-HIV agent Emtricitabine (**FTC**, trade name: Emtriva®). Specifically, we demonstrate the ability of **FTC** to function as an artificial supramolecular cleft-like receptor of bipyridines (**Scheme 1a**,**b**). The cleft is stabilized by complementary hydrogen bonding and through synthon competition. **FTC** is a major anti-HIV drug approved by the FDA included in the World Health Organization (WHO)'s List of Essential Medicines.[3]

Seminal work by Rebek described the ability of *single molecules* to function as molecular clefts that recognize linear rod-shaped guests (**Scheme 1c**).[4] Recognition is achieved owing to convergent hydrogen-bond donor sites. **FTC** self-assembles as a homodimer in the solid state, with axial hydroxyl groups engaged in N-H···N hydrogen bonds in a *transoid* conformation (**Figure S1**, ESI).[5] Cocrystals of **FTC** are unknown, thus, as part of our program of study of multi-component solids,[6] we asked whether **FTC** would form cocrystals with the rod-shaped bipyridines 1,2-bis(4-pyridyl)ethane (**bpeta**), 1,2-bis(4-pyridyl)ethylene (**bpe**), 4,4'-azopyridine (**apy**), and 4,4'-bipyridine (**bipy**). During our research, we discovered N-H···N hydrogen bonding of **FTC** to enable **FTC** to function as a self-assembled (i.e. supramolecular) cleft that recognizes **bpeta**, **bpe** and **apy**. The binary solids form an isostructural set of cocrystals. We are unaware of a case wherein the behaviour of a unimolecular cleft has been expressed supramolecularly.

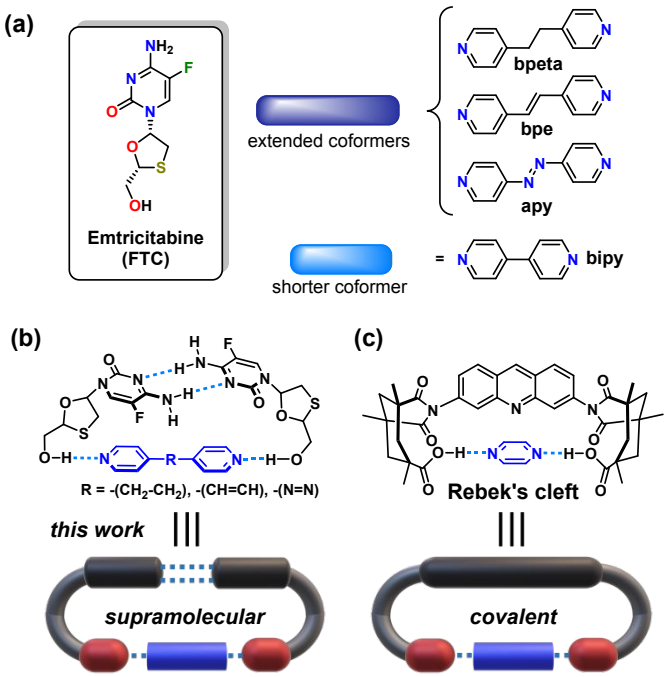

Scheme 1. (**a**) **FTC** and 4-pyridyl-containing coformers, (**b**) supramolecular cleft recognition, and (**c**) cleft recognition.

Department of Chemistry, University of Iowa, Iowa City, IA, 52242, USA. E-mail: len-macgillivray@uiowa.edu; Tel: (+1) 319 335 3504

Electronic Supplementary Information (ESI) available: CCDC 1981473–1981476 Experimental conditions, powder X-ray diffractograms, additional SCXRD data. See DOI: 10.1039/x0xx00000x

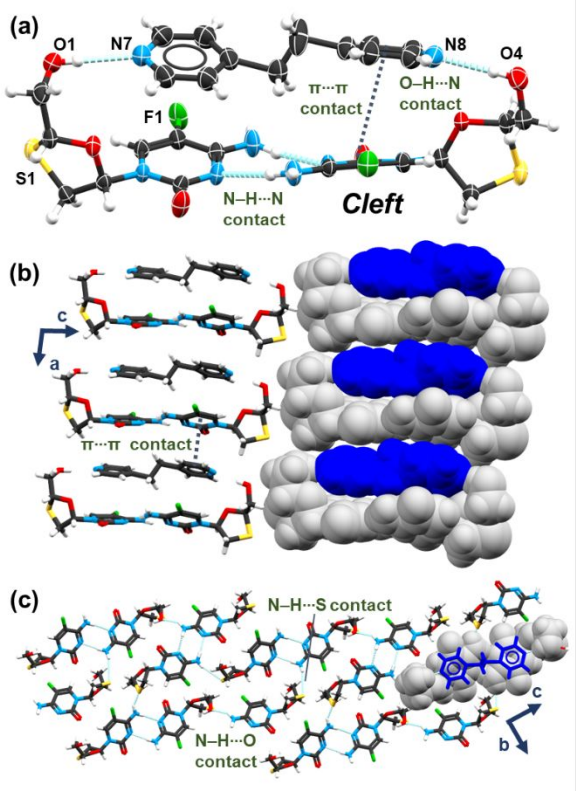

Figure 1. X-ray structure (**FTC**)$_2$·(**bpeta**): (**a**) three-component assembly, (**b**) 1D parallel columns, (**c**) ribbons.

Initially, **FTC** (40 mg, 0.162 mmol) was combined with **bpeta** (14.9 mg, 0.081 mmol) through liquid-assisted grinding (LAG, methanol)[7] for 15 min. Powder X-ray diffraction (PXRD) revealed a new solid phase by the appearance of a new set of peaks (e.g., prominent peaks at 2θ = 11.7, 15.7, 16.5 and 24.9°) when compared to the staring materials (**Figure S3**, ESI). Recrystallization of the solid in warm methanol (2 mL) afforded single crystals suitable for single-crystal X-ray diffraction (SCXRD) after slow evaporation over a period of 2 days. The composition of the solid was (**FTC**)$_2$·(**bpeta**) by ^{1}H NMR spectroscopy (**Figures S7-S11**, ESI) and SCXRD (**Table 1**). PXRD confirmed the solid phases to agree with those of grounded solids. The LAG was necessary to form the solid phases.[8]

Structural analysis of (**FTC**)$_2$·(**bpeta**) revealed the components to assemble in the monoclinic space group $P2_1$. **FTC** adopts a J-shape conformation and assembles into homodimers through N-H···N hydrogen bonds (**Table S2**, ESI).[5,9] The orientation of the NH_2 groups is also sustained by weak intramolecular N-H···F hydrogen bonds similarly to structurally related molecules.[10] The formation of the homodimers results in two the terminal hydroxyl groups adopting a *cisoid*, or convergent, orientation (O···O separation: 14.676(5) to 14.951(4) Å]. The hydroxyl groups interact with **bpeta** through O-H···N_{pyr} hydrogen bonds to generate a discrete three-component assembly (**Figure 1a**). The *cisoid* disposition of the hydroxyl groups contrasts a *transoid* orientation in pure **FTC**.[5] The **FTC** molecules, thus, effectively chelate[11] **bpeta** as a supramolecular linker. Cocrystal formation is further stabilized by π···π contacts between the 5-fluorocytosine rings and bipyridines.[12] The assemblies form columns that run along the *a*-axis in an (ABA)$_n$ pattern (A= **FTC**, B= **bpeta**) sustained by π···π contacts. C-H···S contacts support parallel alignment of the columns in the *ac*-plane (**Figure 1b**).[13] The columns define a herringbone arrangement in the *bc*-plane facilitated by N-H···S and N-H···O contacts (**Figure 1c**).

Table 1. Crystallographic data (**FTC**)$_2$·(**bpeta**), (**FTC**)$_2$·(**bpe**), (**FTC**)$_2$·(**apy**), and (**FTC**)$_2$·(**bipy**)$_2$·**H$_2$O**

crystal data[a]	(**FTC**)$_2$·(**bpeta**)	(**FTC**)$_2$·(**bpe**)	(**FTC**)$_2$·(**apy**)	(**FTC**)$_2$·(**bipy**)$_2$·**H$_2$O**
chemical formula	$(C_8H_{10}FN_3O_3S)_2$ ·$(C_{12}H_{12}N_2)$	$(C_8H_{10}FN_3O_3S)_2$ ·$(C_{12}H_{10}N_2)$	$(C_8H_{10}FN_3O_3S)_2$ ·$(C_{12}H_8N_4)$	$(C_8H_{10}FN_3O_3S)_2$·$(C_{10}H_8N_2)_2$·H_2O
MW (gmol^{-1})	678.73	676.72	677.69	824.895
space group	$P2_1$	$P2_1$	$P2_1$	$P2_1$
a (Å)	7.6333(8)	7.4883(7)	7.5024(8)	7.4668(10)
b (Å)	11.2359(11)	11.2957(11)	11.2194(11)	9.6700(14)
c (Å)	18.1058(18)	18.1735(18)	18.2134(18)	26.187(4)
α (deg)	90	90	90	90
β (deg)	99.640(5)	100.406(5)	100.538(5)	90.087(4)
γ (deg)	90	90	90	90
V (Å^3)	1531.0(3)	1511.9(3)	1507.2(3)	1890.8(5)
Z	2	2	2	2
μ (mm^{-1})	0.243	0.246	0.249	0.215
ρ_{calcd} (gcm^{-3})	1.472	1.486	1.493	1.449
R_1[b,c]	0.0292	0.0369	0.0487	0.0559
wR_2[d,e]	0.0700	0.0869	0.1157	0.1307
CCDC	1981473	1981474	1981475	1981476

[a]$\lambda_{MoK\alpha}$ = 0.71073 Å. [b]$F_o > 2\sigma(F_o)$. [c]$R_1 = \sum|F_o|-|F_c|/\sum|F_o|$. [d]All data. [e]$wR_2 = [\sum w(F_o^2 - F_c^2)^2/\sum w(F_o^2)^2]^{1/2}$

Tolerance of the cleft-like behavior of **FTC** is evidenced by cocrystals (**FTC**)$_2$·(**bpe**) and (**FTC**)$_2$·(**apy**) (**Figures 2a,b**). The solids, both of which are isostructural to (**FTC**)$_2$·(**bpeta**), formed by LAG (methanol) as confirmed by PXRD analysis (**Figures S4-S6**, ESI). Single crystals suitable for SCXRD were obtained by recrystallization of the solids in warm methanol. The resulting clefts effectively "shrink-wrap" to accommodate the different bipyridines (**Table 2**).[14] Thus, there is variability in spacer lengths (N···N 9.024(5) to 9.395(4) Å), which is then reflected in the hydroxyl group separations (O···O 14.676(5) to 14.951(4) Å) across the clefts. The three isostructural solids exhibit a mutual crystal packing similarity index of 99.3% (**Figure 2c**).[15] UNI intermolecular potentials[16] of isostructural cocrystals indicated a small variability in the total packing energies (ΔE_{TOT} = 11 kJ mol^{-1}), being (**FTC**)$_2$·(**apy**) and (**FTC**)$_2$·(**bpeta**) the lowest and highest energy packings (**Table S3**, ESI).

An 'error' occurs in the self-assembly when **FTC** is introduced to the slightly smaller bipyridine **bipy** (**Figure 3**). The components form the cocrystal hydrate (**FTC**)$_2$·(**bipy**)$_2$·**H$_2$O** by LAG (methanol). Recrystallization of the solid in warm methanol afforded single crystals in the monoclinic space group $P2_1$ (**Table S1**, ESI). **FTC** forms a hydrogen-bonded catemer (**Figure 3a**) wherein the API, similar to pure **FTC**, adopts the *transoid* conformation (**Figure 3a**).[17] As a consequence of the assembly process, the components form 1D ribbons along the *c*-axis in an

$(ABCCB)_n$ pattern (A= **H_2O**, B= **bipy**, C= **FTC**). Adjacent ribbons interact by π-stacking of **bipy** along the *a*-axis (**Figure 3b**). We attribute the formation of the ribbons to the shorter distance of the **bipy** guest (N···N 7.093(6), 7.117(8)). It is likely that the shorter length circumvents **bipy** to offer an element of preoganization to cleft formation, and thus allows a more efficiently packed hydrogen-bonded hydrated structure to form (**Table S3**, ESI)

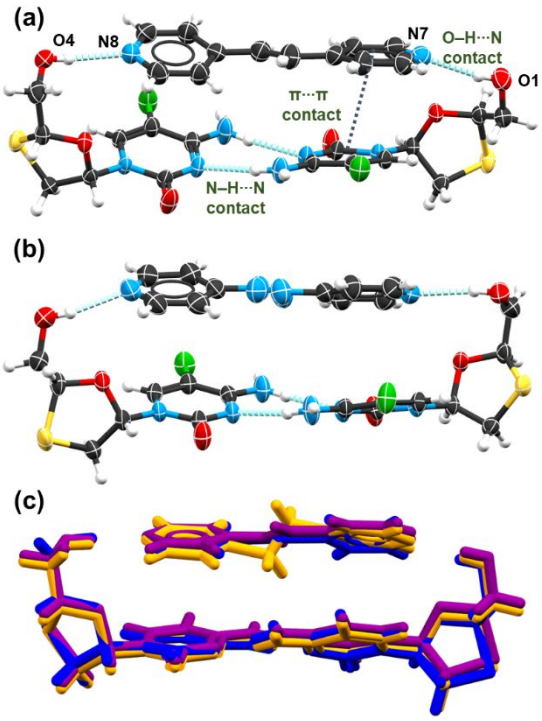

Figure 2. X-ray structures: (**a**) $(FTC)_2$·(**bpe**), (**b**) $(FTC)_2$·(**apy**), and (**c**) overlay of $(FTC)_2$·(**bpe**) (purple), $(FTC)_2$·(**apy**) (blue), and $(FTC)_2$·(**bpeta**) (orange).

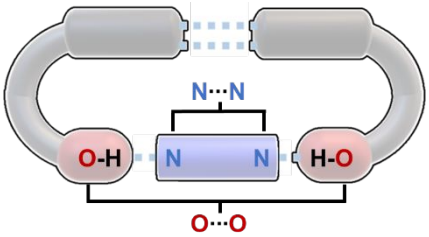

Scheme 2. Selected metrics in $(FTC)_2$·(**bpeta**), $(FTC)_2$·(**bpe**) and $(FTC)_2$·(**apy**).

Table 2. O-H···N_{pyr} hydrogen-bonds and selected π···π interactions of $(FTC)_2$·(**bpeta**), $(FTC)_2$·(**bpe**), $(FTC)_2$·(**apy**) and $(FTC)_2$·(**bipy**)$_2$·H_2O.

Cocrystal	*d*O-H···N (Å)	*d*O···O (Å)	*d*N···N (Å)
$(FTC)_2$·(**bpeta**)	2.838(4), 2.850(4)	14.889(4)	9.359(4)
$(FTC)_2$·(**bpe**)	2.863(4), 2.858(4)	14.951(4)	9.395(4)
$(FTC)_2$·(**apy**)	2.895(5), 2.887(5)	14.676(5)	9.024(5)

In this contribution, we have described supramolecular repurposing of the anti-HIV drug **FTC.** The API acts as a supramolecular cleft for bipyridine recognition in the solid state. Having identified the hydrogen-bonding recognition capabilities of **FTC**, we envisage possible supramolecular repurposing of other APIs,[18] and similar molecules lined with multiple functional groups, to enable the formation of solids that exhibit additional properties (e.g., photoactive,

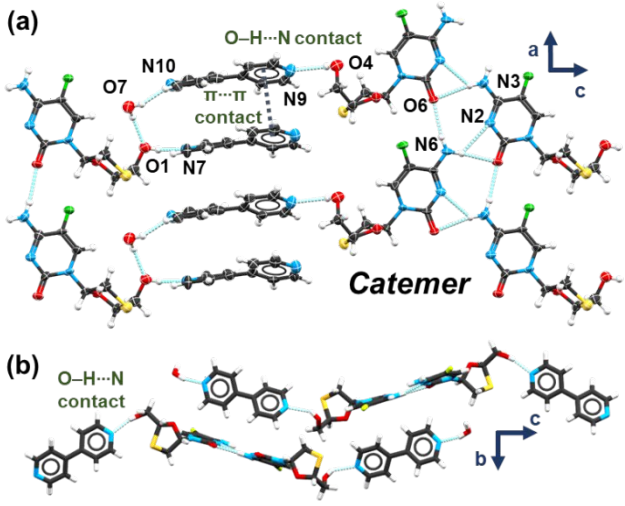

semiconductors, storage, separation).[19]

Figure 3. X-ray structure $(FTC)_2$·(**bipy**)$_2$·H_2O: (**a**) hydrogen bonding and (**b**) adjacent 1D ribbons.

Acknowledgements

The authors acknowledge financial support from the National Science Foundation (DMR-1708673). G.C.-A. acknowledges financial support from CONACYT-COVEICYDET.

Conflicts of interest

There are no conflicts to declare.

References

1. (a) J. A. DiMasi, H. G. Grabowski and R. W. Hansen, *J. Health Econ.*, 2016, **47**, 20-33; (b) S. Pushpakom, F. Iorio, P. A. Eyers, K. J. Escott, S. Hopper, A. Wells, A. Doig, T. Guilliams, J. Latimer, C. McNamee, A. Norris, P. Sanseau, D. Cavalla and M. Pirmohamed, *Nat. Rev. Drug Discov.*, 2019, **18**, 41-58.
2. F. Zhang, V. Lemaur, W. Choi, P. Kafle, S. Seki, J. Cornil, D. Beljonne and Y. Diao, *Nat. Commun.*, 2019, **10**, 4217.
3. J. E. Gallant, E. DeJesus, J. R. Arribas, A. L. Pozniak, B. Gazzard, R. E. Campo, B. Lu, D. McColl, S. Chuck, J. Enejosa, J. J. Toole and A. K. Cheng, *N. Engl. J. Med.*, 2006, **354**, 251-260.
4. (a) J. Rebek, B. Askew, M. Killoran, D. Nemeth and F. T. Lin, *J. Am. Chem. Soc.*, 1987, **109**, 2426-2431; (b) J. Rebek and D. Nemeth, *J. Am. Chem. Soc.*, 1986, **108**, 5637-5638; (c) J. Rebek Jr, B. Askew, N. Islam, M. Killoran, D. Nemeth and R. Wolak, *J. Am. Chem. Soc.*, 1985, **107**, 6736-6738; (d) L. R. MacGillivray, M. M. Siebke and J. L. Reid, *Org. Lett.*, 2001, **3**, 1257-1260; (e) D. B. Varshney, X. Gao, T. Friščić and L. R. MacGillivray, *Angew. Chem. Int. Ed.*, 2006, **45**, 646-650; (f) M. Harder, M. A. Carnero Corrales, N.

Trapp, B. Kuhn and F. Diederich, *Chem. Eur. J.*, 2015, **21**, 8455-8463.

5. P. van Roey, W. A. Pangborn, R. F. Schinazi, G. Painter and D. C. Liotta, *Antiviral Chem. Chemother.*, 1993, **4**, 369-375.
6. (a) G. Campillo-Alvarado, T. Didden, S. Oburn, D. C. Swenson and L. R. MacGillivray, *Cryst. Growth Des.*, 2018, **18**, 4416-4419; (b) G. Campillo-Alvarado, C. A. Staudt, M. J. Bak and L. R. MacGillivray, *CrystEngComm*, 2017, **19**, 2983-2986; (c) G. Campillo-Alvarado, C. Li, D. C. Swenson and L. R. MacGillivray, *Cryst. Growth Des.*, 2019, **19**, 2511-2518; (d) G. Campillo-Alvarado, A. D. Brannan, D. C. Swenson and L. R. MacGillivray, *Org. Lett.*, 2018, **20**, 5490-5492.
7. S. Karki, T. Friščić, W. Jones and W. D. S. Motherwell, *Mol. Pharm.*, 2007, **4**, 347-354.
8. (a) A. V. Trask and W. Jones, in *Organic Solid State Reactions*, ed. F. Toda, Springer Berlin Heidelberg, Berlin, Heidelberg, 2005, pp. 41-70; (b) R. Kuroda, Y. Imai and N. Tajima, *Chem. Commun.*, 2002, 2848-2849; (c) A. V. Trask, J. van de Streek, W. D. S. Motherwell and W. Jones, *Cryst. Growth Des.*, 2005, **5**, 2233-2241; (d) P. M. Bhatt, Y. Azim, T. S. Thakur and G. R. Desiraju, *Cryst. Growth Des.*, 2009, **9**, 951-957; (e) L. Rajput, P. Sanphui and G. R. Desiraju, *Cryst. Growth Des.*, 2013, **13**, 3681-3690; (f) C. C. da Silva and F. T. Martins, *J. Mol. Struct.*, 2019, **1181**, 157-170.
9. (a) J. P. Jasinski, R. J. Butcher, L. Mallesha, K. Mohana, H. Yathirajan and B. Narayana, *J. Chem. Crystallogr.*, 2009, **39**, 433-437; (b) M. Cetina, K. Benci, K. Wittine and M. Mintas, *Cryst. Growth Des.*, 2012, **12**, 5262-5270; (c) J. d. C. Fonseca, J. C. Tenorio Clavijo, N. Alvarez, J. Ellena and A. P. Ayala, *Cryst. Growth Des.*, 2018, **18**, 3441-3448.
10. A. Jaworski, M. Szczesniak, K. Szczepaniak, K. Kubulat and W. B. Person, *J. Mol. Struct.*, 1990, **223**, 63-92.
11. J. Rebek, *Acc. Chem. Res.*, 1990, **23**, 399-404.
12. J. C. Tenorio, R. S. Corrêa, A. A. Batista and J. Ellena, *J. Mol. Struct.*, 2013, **1048**, 274-281.
13. (a) I. S. Antonijević, G. V. Janjić, M. K. Milčić and S. D. Zarić, *Cryst. Growth Des.*, 2016, **16**, 632-639; (b) M. K. Krepps, S. Parkin and D. A. Atwood, *Cryst. Growth Des.*, 2001, **1**, 291-297.
14. (a) K. T. Holman, A. M. Pivovar, J. A. Swift and M. D. Ward, *Acc. Chem. Res.*, 2001, **34**, 107-118; (b) J. Pitchaimani, A. Kundu, S. Karthikeyan, S. P. Anthony, D. Moon and V. Madhu, *CrystEngComm*, 2017, **19**, 3557-3561.
15. R. de Gelder, R. Wehrens and J. A. Hageman, *J. Comput. Chem.*, 2001, **22**, 273-289.
16. (a) A. Gavezzotti, *Acc. Chem. Res.*, 1994, **27**, 309-314; (b) A. Gavezzotti and G. Filippini, *J. Phys. Chem.*, 1994, **98**, 4831-4837.
17. N. Variankaval, C. Lee, J. Xu, R. Calabria, N. Tsou and R. Ball, *Org. Process Res. Dev.*, 2007, **11**, 229-236.
18. S. M. Corsello, J. A. Bittker, Z. Liu, J. Gould, P. McCarren, J. E. Hirschman, S. E. Johnston, A. Vrcic, B. Wong, M. Khan, J. Asiedu, R. Narayan, C. C. Mader, A. Subramanian and T. R. Golub, *Nat. Med.*, 2017, **23**, 405-408.
19. E. A. Wintner, M. M. Conn and J. Rebek, *J. Am. Chem. Soc.*, 1994, **116**, 8877-8884.

Table of Contents Figure

Supramolecular repurposing of the anti-HIV drug Emtricitabine enables the recognition of rod-shaped bipyridines as a hydrogen-bonded supramolecular cleft.